

JET-NOISE CONTROL BY FLUIDIC INJECTION FROM A ROTATING PLUG: LINEAR AND NON-LINEAR SOUND SOURCE MECHANISMS

M. Koenig

Acoustics Department
SNECMA, SAFRAN Group
Moissy-Cramayel, FRANCE
maxime.koenig@etu.univ-poitiers.fr

A.V.G. Cavalieri

Laboratório de Engenharia Aeronáutica
Instituto Tecnológico de Aeronáutica
São José dos Campos, SP, BRAZIL
andre@ita.br

P. Jordan, Y. Gervais

Département Fluides, Thermique et Combustion
Institut Pprime
CEAT, Poitiers, FRANCE
peter.jordan@univ-poitiers.fr, yves.gervais@univ-poitiers.fr

ABSTRACT

We present a study of subsonic jets, controlled by means of a novel actuator that introduces perturbations via steady fluidic actuation from a rotating centerbody (Koenig *et al.* (2011a)). Preliminary results obtained with this kind of actuator were presented during AIAA conference in Portland in 2011 (Koenig *et al.* (2011b)). Louder and quieter jets are produced, and these are analysed using time-resolved, stereoscopic particle image velocimetry and a hot-wire anemometer. We place the analysis in the framework of wavepackets and linear stability theory, whence we show that the quieter flows can be understood to result from a mean-flow deformation that attenuates wavepacket growth rates. The mean-flow deformation is shown, by a triple decomposition, to be due to the generation of Reynolds stresses associated with incoherent turbulence (rather than coherent structures) which arises when the actuation energises the flow with a frequency—azimuthal wavenumber ($\omega - m$) combination to which the mean flow is stable. When the actuation energises the flow with an $\omega - m$ combination to which the mean flow is unstable, the response is dominated by coherent structures, whose rapid growth takes them beyond the linear limit where they undergo quadratic wave interactions and, consequently, a louder flow.

INTRODUCTION

We know that jet noise can be manipulated, enhanced or reduced, through a modification of the flow conditions in the vicinity of the nozzle exit. The modification may be due to a change in the geometry of the nozzle, using tabs or chevrons for instance (Zaman *et al.* (2011)), or non-circular nozzles (Gutmark & Grinstein (1999)). It may result from the addition of mass and momentum via steady fluidic injection (Henderson (2010)). But the synthesis, and/or ‘optimisation’ of, noise-reduction strategies remains problematic, being either guided by trial and error or based on the laborious exploration of hopelessly large parameter spaces. In the latter scenario partial automation may sometimes be possible (Maury *et al.* (2012)).

The limited success of noise control strategies can be attributed to the lack of a solid conceptual framework connecting perturbations near the nozzle to the sound energy radiated to the farfield, one which would enable a clear interpretation of the control effect, and thereby provide physics-based guidance through the myriad actuation possibilities.

Unsteady actuation, produced for instance by fluidic pulsing (Maury *et al.* (2011)) or plasma discharge (Samimy *et al.* (2007)), is a means by which perturbations can be imposed in a more controlled fashion at the nozzle: a well-defined frequency and azimuthal mode combination can be introduced and the response of the flow (turbulence and sound) assessed with that knowledge. This is in contrast to the aforementioned steady-fluidic techniques, where the frequency-wavenumber structure of the near-nozzle perturbation is largely governed by the turbulence resulting from the interaction between the main jet and the injected fluid.

Furthermore, noise-controlled flows produced by unsteady actuation, be they louder or quieter, provide a useful setting for the development of understanding regarding that conceptual framework that would link actuation to sound. In this paper we present a novel actuator, partial results were presented during AIAA conference in Portland in 2011 (Koenig *et al.* (2011b)), that produces an unsteady fluidic perturbation in the near-nozzle region of a round jet. Depending on the frequency-wavenumber structure of the perturbation, the actuator can produce louder or quieter jets with respect to the baseline; the study enables a rather complete analysis and interpretation of both control effects, and in this it goes some way towards validating the conceptual framework we use, which consists in considering hydrodynamic wavepackets, understood as instabilities of the turbulent mean flow, to comprise the main sound-producing flow activity.

EXPERIMENTAL SETUP

The experiments were performed in the PPRIME Institute anechoic jet noise facility, “Bruit et Vent”, at the CEAT, Poitiers. An isothermal jet issuing from a round nozzle with

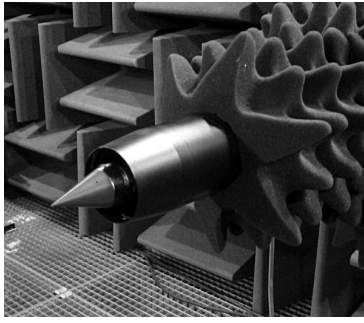


Figure 1: Rotating plug actuator in “Bruit et Vent”.

a plug is studied. The exit Mach number is varied from 0.3 to 0.6, but on account of limitations in the rotation speeds possible with the actuator, the main results reported here are for the $M=0.3$ case. The nozzle diameter, $D_{\text{jet}}=0.05$ m, and a plug (centerbody) of diameter $D_{\text{plug}}=0.03$, mounted in the centre of the jet (see figure 1), is driven in rotation by an electric motor. Air is injected into the plug via a hole in the crankshaft. The air is ejected at 240 m/s into the main jet by two diametrically opposed control ports of diameter 0.0013 m. The control-jet flow rate is less than 0.5% that of the main jet. An equivalent diameter, D , is defined as $D = \sqrt{D_{\text{jet}}^2 - D_{\text{plug}}^2}$. This leads to an equivalent diameter $D = 0.04$ m. This diameter is used as the reference length of the flow and gives a Reynolds number, $Re_D = U_j D / \nu = 2.7 \times 10^5$.

Microphone measurements were made at 30 diameters (D) from the jet, at downstream angles of 20° and 30° . A moving average was used to smooth the spectra, and peaks associated with sound radiated by the electric motor have been removed by a notch filter in the results presented here.

Velocity measurements were made using a LaVision time-resolved Stereoscopic PIV system and cameras with 1024×1024 pixel resolution. The light source was a 10 mJ Quantronix Darwin duo laser (light sheet thickness 2 mm) and the flow was seeded with oil smoke. Three components of velocity were measured in $r - \theta$ planes at a range of axial stations by two SA1 Photron cameras. The sampling frequency was 2.7 kHz. 10000 PIV image pairs were recorded, this being sufficient for convergence of first and second order statistical moments. Image-processing consisted of a five-pass correlation routine with 64×64 pixel correlation for the first pass, 16×16 pixel for the final pass and with a 50% correlation overlap at each pass. The spatial resolution was one velocity vector every 0.75 mm for the small window size (near the jet exit) and one velocity vector every 1.5 mm for the large window size (around the end of the potential core). Hot-wire measurements are also presented in this paper to evaluate the mixing layer close to the plug extremity. We use a single hot-wire ($2.5 \mu\text{m}$), sampled at 250 kHz. An in-situ calibration of the hot-wire is performed as in Tutkun *et al.* (2009). This time, only the axial component of the velocity is captured by the hot wire in $x - r$ planes.

The perturbation introduced by the actuator is dominated, on account of the actuator geometry, by an azimuthal mode 2, and a frequency equal to twice the rotation frequency: $f_p = 2f_{\text{rotation}}$; a perturbation Strouhal number is defined as $St_p = f_p D / U_j$.

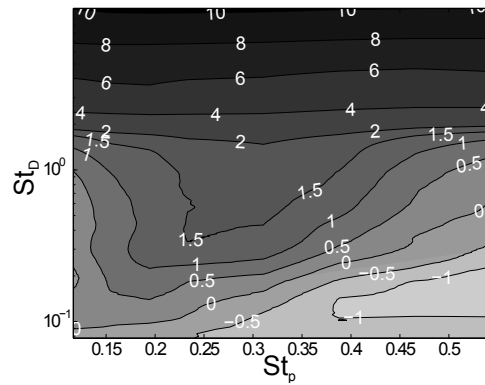


Figure 2: Change in noise baseline vs controlled jet (contours in dB) as a function of perturbation Strouhal number and Strouhal number at 20° and Mach 0.3.

ACOUSTIC RESPONSE

The injection flow rate and plug rotation frequency are the two controlling parameters. These were assessed for different main-jet Mach numbers and the analysis indicates that, while similar noise reductions are probable at higher Mach number, the rotation-frequency limit constrains us to study the Mach 0.3 jet. We therefore focus on this jet, at a fixed injection flow rate (around 0.5%), and we explore the acoustic response of the system as a function of the perturbation frequency.

The result, summarised in figure 2, has three features of note. A high-frequency noise increase is observed at $St_D > 2$. This is associated with scattering, by the plug, of turbulence associated with the fluidic injection: we have established that this component of the noise has a lower velocity scaling than the jet noise, and is no longer measurable at higher Mach number. The second feature of interest is the monotonic increase, with perturbation frequency, of the cross-over frequency between noise reduction and noise increase. Future studies, using a new, more rapid, prototype will establish if this trend continues. The third feature, and which constitutes the main focus of this paper, is the difference between the louder jet, observed when the actuator is driven at a rotation frequency of $St_D = 0.23$, and the quieter jets, typified by that obtained when the actuator is driven at $St_D = 0.46$. The analysis of the flow will thus focus on these two perturbation Strouhal numbers.

AERODYNAMIC RESPONSE

Some global indicators of the flow response to actuation are shown in figure 3. The mean field deformation in the near nozzle region is similar at both rotation frequencies, except on the centerline, where a monotonic increase in mean velocity is observed with increasing actuation frequency. Farther downstream the behaviour is non-monotonic if the baseline case is included as a zero-frequency case: as the frequency is increased, the mean flow first spreads and then retracts, but remains always broader than the baseline field.

The centerline profile, shown in figure 3(b), illustrates this difference between the near-plug region and the downstream region: changes are monotonic with frequency up to about $x/D=5$, downstream of which the trend is non-monotonic. We note, nonetheless, that the two controlled

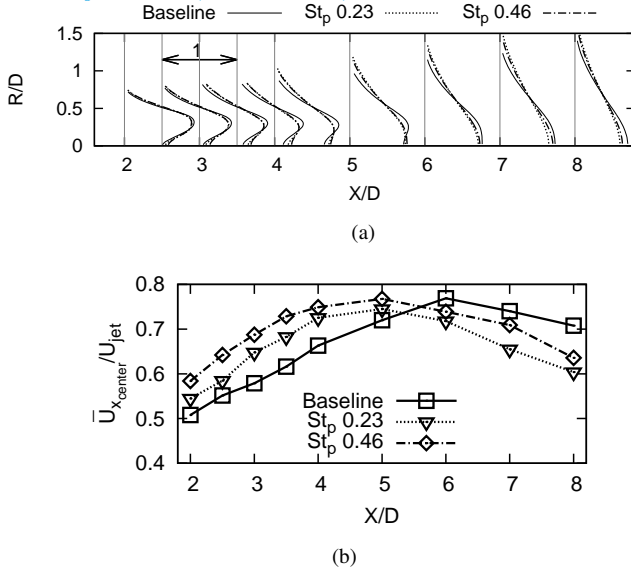


Figure 3: (a) Mean axial velocity \bar{U}_x/U_j ; (b) Longitudinal evolution of centerline mean axial velocity.

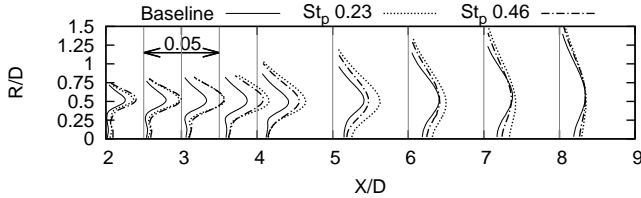


Figure 4: Turbulent kinetic energy profile.

profiles have similar shapes: both entrain and redistribute axial momentum toward the centerline in the initial region, this effect being enhanced when the rotation frequency is increased. Other global indicators, such as the entrainment, show similar behaviour.

The turbulent kinetic energy (hereafter TKE), which can be observed in figures 4 is similarly enhanced at both frequencies in the near-nozzle region, whereas downstream of $x/D=3$, after a large increase at $St_D = 0.23$ it decreases at $St_D = 0.46$ to the point where the peak levels drop below that of the baseline downstream of $x/D = 6$. This normal components of the Reynolds stress tensor (not shown) show a similar behaviour, indicating that the energisation is more or less isotropic.

In what follows, an analysis of the (ω, m) structure of the near-plug TKE will help to understand the very different axial evolutions of the fluctuation energy in the two cases: both flows are equally energised, but with quite different spatiotemporal characteristics, provoking, as a consequence, quite different responses in the downstream region, from which sound emission is greatest.

ANALYSIS AND INTERPRETATION

The quieter flow

Hypothesis I: an attenuated axisymmetric wavepacket

We first consider the quieter, $St_p=0.46$, case, and note that the greatest noise reduction is observed at low emission

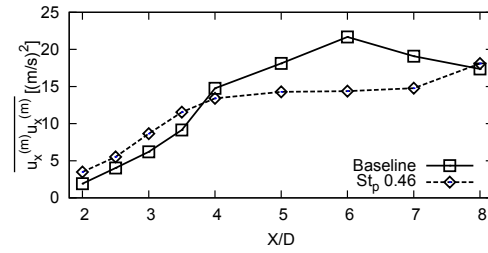


Figure 5: Axial evolution of fluctuating energy of the axisymmetric component of the axial velocity.

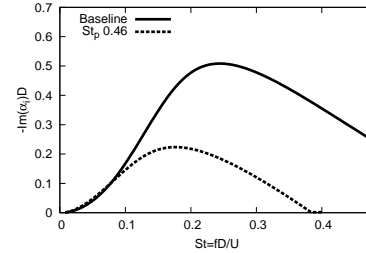


Figure 6: Growth rates of azimuthal mode, $m=0$, as a function of frequency, for baseline and $St_p = 0.46$ actuation at $X = 4D$.

angles, where the sound field is known to be predominantly axisymmetric (Kopiev *et al.* (2010), Cavalieri *et al.* (2012), Juvé *et al.* (1979)), and dominated by a source mechanism driven by the axisymmetric component of the axial velocity fluctuation (Cavalieri *et al.* (2012)). This sound source is considered by many (Jordan & Colonius (2012)) to comprise an axially-extended, non-compact wavepacket, understood as an instability of the mean field. We therefore begin the interpretation with the hypothesis that the noise reduction is associated with a reduction of the fluctuation energy of the axial velocity component of an axisymmetric wavepacket. The fluctuation energy of the axisymmetric component, provided by a Fourier-series decomposition of the TR-PIV data, and shown in figure 5, validates the above hypothesis: downstream of $x/D=4$ reductions of up to 25% are observed.

Hypothesis II: reduced instability growth rates

The second hypothesis is that the reduction in the axisymmetric fluctuation energy results from a change in the growth rates of linear instabilities, this being due to the mean-field deformation produced by the actuation. A linear stability analysis, based on the parallel-flow assumption (Michalke (1971)), is performed using the mean velocity profiles. The result is shown in figure 6 for the axisymmetric component of the axial velocity. For the frequency range over which a noise reduction is achieved $St_D < 0.25$ we see that, downstream of $x/D=3$ —which is where the reduction in axisymmetric fluctuation energy is observed—the growth rates have been considerably suppressed. The second hypothesis is thus verified.

We now try to understand the mean-flow deformation by considering the mean momentum balance for the axial velocity component, written in terms of a triple decomposition of the axial velocity, $u = \bar{U} + \bar{u} + u'$,

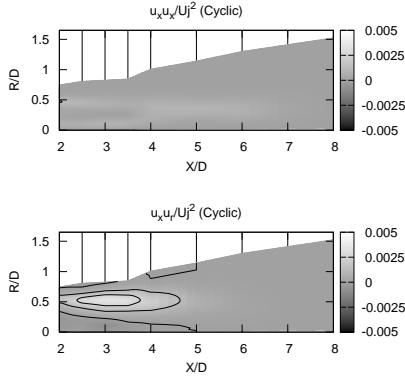


Figure 7: Contribution of cyclic components in the Reynolds stress tensor comparatively to baseline jet for (up) $u_x' u_x'$ and (down) $u_r' u_r'$.

$$\rho_0 \left(\bar{U}_x \frac{\partial \bar{U}_x}{\partial x} + \bar{U}_r \frac{\partial \bar{U}_x}{\partial r} \right) = -\frac{\partial \bar{P}}{\partial x} + \mu \bar{S}_x - \rho_0 \left(\frac{\partial (\bar{u}_x'^2 + \bar{u}_r'^2)}{\partial x} + \frac{1}{r} \frac{\partial (r \bar{u}_x' \bar{u}_r' + r \bar{u}_r' \bar{u}_x')}{\partial r} \right).$$

The deformation of the mean field is due to both coherent and incoherent Reynolds stresses, the former being associated with coherent structures (or wavepackets), the latter with background turbulence. We look at the contribution of each in order to get a sense of how the actuation produced the mean-field deformation. Figure 7 shows maps of the difference between the Reynolds stresses of the baseline and the controlled flows; the components shown are those that participate in the axial mean momentum balance, $u_x' u_x'$ and $u_r' u_r'$. The figure shows that the mean-field deformation is dominated by the non-cyclic components of the Reynolds stress. The cyclic component, associated with the organised, wavepacket component of the response, is small, indicating that the *response of the flow to the high-frequency actuation comprises turbulence rather than coherent structures*.

Hypothesis III: actuation at stable (ω, m)

The above observation leads to the following, third, hypothesis: the dynamics of the flow response to actuation is primarily comprised of incoherent turbulence *because the actuation energises the flow with an (ω, m) structure to which the mean-field is stable*. A linear stability analysis shows (cf. figure 8) that the mean field is indeed everywhere stable to the actuation structure ($St_p = 0.46, m = 2$); and so we conclude that the considerable fluctuation energy introduced into the system by the actuation at azimuthal mode $m = 2$ (cf. figure 9), evolves downstream as incoherent turbulence, producing a mean-field deformation on which axisymmetric linear waves, which dominate downstream radiation, have lower growth rates.

With this we have a self-consistent phenomenological interpretation linking the actuation to the farfield and the analysis of the quieter flow is complete. We note that the results of a number of other jet noise control studies are consistent with this: noise abatement is most efficient when flows are driven with high $\omega - m$ combinations (Samimy *et al.* (2007), Kopiev *et al.* (2010)). While we cannot affirm

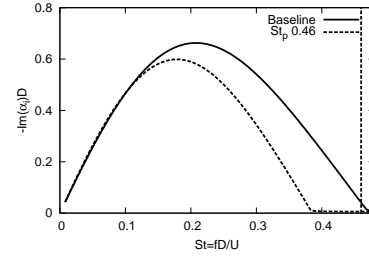


Figure 8: Growth rates of azimuthal mode, $m = 2$, as a function of frequency, for baseline and $St_p = 0.46$ actuation at $X = 2D$. The dotted vertical line shows the perturbation frequency.

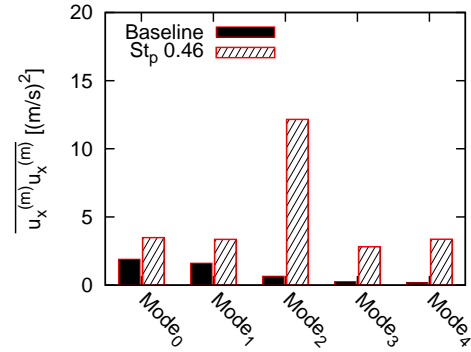


Figure 9: Fluctuation energy of azimuthal modes of the axial velocity component in the near-plug region ($x/D=2$) at $R=0.25D$ (where peak levels are observed).

that the mean-fields are in those cases stable to such actuation, this does seem likely, as the canonical mean field of a round subsonic jet is most stable to high frequencies and high azimuthal wavenumbers.

In the next section we consider the louder flow in a similar framework, but find that the behaviour is in this case fundamentally different.

The louder flow

Figure 10 compares the fluctuation energy of azimuthal mode $m = 0$ between the baseline and louder flows. In this case we see a slight global increase of the former. Application of the triple decomposition here shows that, contrary to the $St_p = 0.46$ case, that most of the fluctuation energy is contained in the cyclic component. Figure 11, which shows six frames of the phase-averaged field over one complete period, reveals a pattern that repeats twice during that period: a frequency doubling appears to occur, indicating a quadratic wave interaction between the fundamental frequency and itself.

This is confirmed by analysis of hot-wire data. Figure 12 shows velocity power spectra of the baseline and controlled flows. These were measured at the center of the mixing-layer at $x/D = 1.5$. In the $St_p = 0.46$ case a large spike is seen at the actuation frequency, but there are no harmonics. In the $St_p = 0.23$ case, on the other hand, we see a large spike at the fundamental frequency, and this is accompanied by a series of harmonics. A bi-coherence analysis shows (cf. figure 13) levels of over 40%

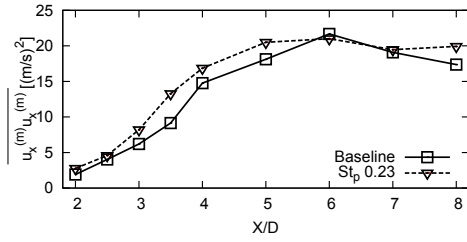


Figure 10: Axial evolution of fluctuating energy of azimuthal mode 0 for the axial velocity component.

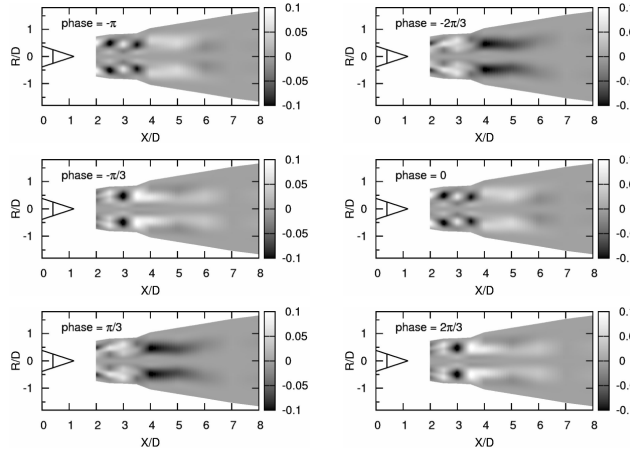


Figure 11: Phase averaged of the axial cyclic component for $St_p = 0.23$ case. Phase is varying from $-\pi$ to $2\pi/3$ by step of $\pi/3$.

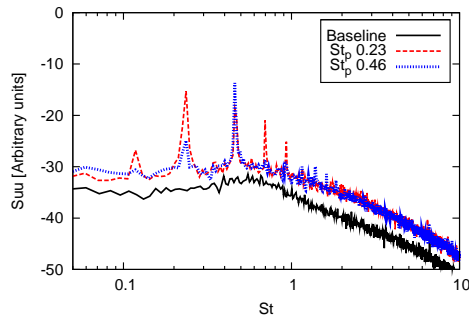


Figure 12: Hot-wire spectra in the mixing layer at $X = 1.5D$ for baseline jet and controlled jets at $St_p = 0.23$ and $St_p = 0.46$.

at $(St, St) = (0.23, 0.23)$ confirming that the first of these harmonics results from a non-linear interaction of the fundamental with itself. *The response of the flow to actuation at the lower frequency is thus seen to comprise non-linear wavepacket dynamics, which are known to be considerably more efficient in the generation of low-angle sound* (Suponitsky et al. (2010)).

Hypothesis IV: non-linear response by energisation at unstable (ω, m)

Finally, with an eye to understanding why the flow responded so differently in this case we formulate and test the

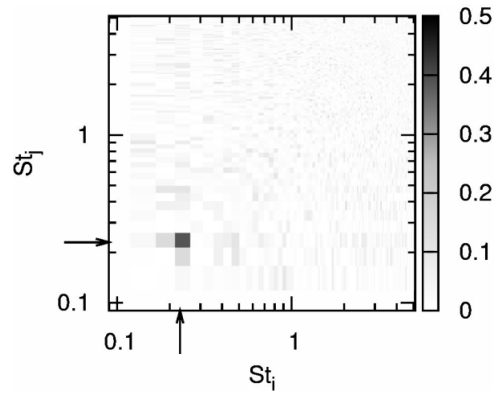


Figure 13: Bicoherence in the mixing layer at $X = 1.5D$ showing non-linear interaction of $St_p = 0.23$ with itself.

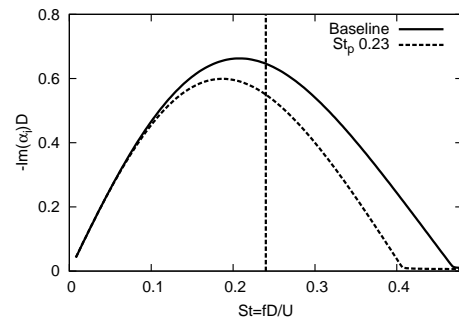


Figure 14: Growth rates, at $x/D = 2$, as a function of frequency for azimuthal mode, $m = 2$, for baseline and $St_p = 0.23$ actuation.

following final hypothesis: the low-frequency actuation introduces high levels of fluctuation energy with an $\omega - m$ structure to which the mean-field is unstable. Figure 14 shows the result of a linear stability analysis, for azimuthal mode, $m = 2$, of both the baseline and actuated mean fields. In both cases we see that the actuation frequency is close to the most unstable frequency of the mean field. This confirms the final hypothesis, and shows, furthermore, that when non-linear wavepacket interactions are present in a subsonic jet, the radiated noise levels are increased above those of the canonical, unforced, flow. This suggests that such quadratic wave interactions do not dominate sound radiation in unforced flows.

CONCLUSIONS

An experimental investigation of subsonic jets subjected to perturbations introduced by means of fluidic injection from a spinning centerbody has been performed. Fluctuation energy is introduced to the flow at azimuthal mode, $m = 2$, and over the perturbation Strouhal number range, $0 < St_p < 0.5$. At low frequency the acoustic response of the flow comprises a noise increase, while at higher frequencies peak noise levels are reduced. The louder and quieter flows are analysed using time-resolved, stereoscopic, particle image velocimetry and a hot-wire anemometer. The high frequency actuation is found to quieten the jet by deforming the mean field such that the growth rates of ax-

isymmetric wavepackets—understood as linear instabilities of the mean flow and which are known to dominate low-angle emission—are reduced. The mean-field deformation is shown, by a triple decomposition, to result from the energisation of incoherent turbulence, which arises because the high frequency actuation introduces fluctuation energy with a $\omega - m$ structure to which the mean field is stable. The louder flow is shown to be due to the excitation of non-linear wavepacket interactions, which arise because at low frequency actuation, the $\omega - m$ structure of the perturbation corresponds to the most unstable frequency of the mean field.

ACKNOWLEDGEMENTS

The present work was supported by SNECMA and CNPq, National Council of Scientific and Technological Development - Brazil.

REFERENCES

- Koenig, M., Vuillemin, A., Jordan, P., Comte, P., and Gervais, Y., (2011a) “Cône arrière de turboréacteur tournant à microjets”, Brevet d’invention (patent) 1154126, INPI.
- Koenig, M., Fourment-Cazenave, C., Jordan, P., and Gervais, Y., (2011b) “Jet noise reduction by fluidic injection from a rotating plug”, 17th AIAA/CEAS Aeroacoustics Conference (32nd AIAA Aeroacoustics Conference).
- Zaman, K., Bridges, J., and Huff, D., (2011) “Evolution from tabs to chevron technology - a review”, *International Journal of Aeroacoustics*, Vol. 10, No. 5, pp. 685–710.
- Gutmark, E. and Grinstein, F., (1999) “Flow control with noncircular jets”, *Annual Review of Fluid Mechanics*, Vol. 31, No. 1, pp. 239–272.
- Henderson, B., (2010) “Fifty years of fluidic injection for jet noise reduction”, *International Journal of Aeroacoustics*, Vol. 9, pp. 91–122.
- Maury, R., Koenig, M., Cattafesta, L., Jordan, P., and Delville, J., (2012) “Extremum-seeking control of jet noise”, *International Journal of Aeroacoustics*, Vol. 11, No. 3, pp. 459–474.
- Maury, R., Cavalieri, A.V.G., Jordan, P., Delville, J., and Bonnet, J., (2011) “Jet noise reduction using pulsed fluidic actuation”, 17th AIAA/CEAS Aeroacoustics Conference (30th AIAA Aeroacoustics Conference).
- Samimy, M., Kim, J.-H., Kastner, J., Adamovich, I., and Utkin, Y., (2007) “Active control of high-speed and high-Reynolds-number jets using plasma actuators”, *Journal of Fluid Mechanics*, Vol. 578, pp. 305–330.
- Tutkun, M., George, W., Foucaut, J., Coudert, S., Stanislas, M., and Delville, J., (2009) “In situ calibration of hot wire probes in turbulent flows”, *Experiments in fluids*, Vol. 46, No. 4, pp. 617–629.
- Kopiev, V., Chernyshev, S., Faranosov, G., Zaitsev, M., and Belyaev, I., (2010) “Correlations of jet noise azimuthal components and their role in source identification”, 16th AIAA/CEAS Aeroacoustics Conference (31st AIAA Aeroacoustics Conference).
- Cavalieri, A.V.G., Jordan, P., Colonius, T., and Gervais, Y., (2012) “Axisymmetric superdirectivity in subsonic jets”, *Journal of Fluid Mechanics*, Vol. 704, pp. 388–420.
- Juvé, D., Sunyach, M., and Comte-Bellot, G., (1979) “Filtered Azimuthal Correlations in the Acoustic Far Field of a Subsonic Jet”, *AIAA Journal*, Vol. 17, No. 1.
- Jordan, P. and Colonius, T., (2012) “Wave Packets and Turbulent Jet Noise”, *Annual Review of Fluid Mechanics*, Vol. 45, No. 1.
- Michalke, A., (1971) “Instabilität eines Kompressiblen Runden Freistrahls unter Berücksichtigung des Einflusses der Strahlgrenzschichtdicke”, *Z. Flugwiss*, English translation: NASA TM 75190, 1977, Vol. 19, pp. 311–328.
- Suponitsky, V., Sandham, N., and Morfey, C., (2010) “Linear and nonlinear mechanisms of sound radiation by instability waves in subsonic jets”, *Journal of Fluid Mechanics*, Vol. 658, pp. 509–538.